

## Article

# Structure Elucidation and Immunoactivity Study of *Armillaria mellea* Fruiting Body Polysaccharides

Qingqing Li, Ying Li, Huazhou Niu, Enhui Wang, Lili Jiao, Hui Li, Wei Wu \*

Jilin Ginseng Academy, Changchun University of Chinese Medicine, Changchun 130117, China; liqqsunny@126.com (Q.L.); ying060111@163.com (Y.L.); niuhuazhou95@163.com (H.N.); wang\_enhui2022@163.com (E.W.); jiaoaj@hotmail.com (L.J.); lihuiterrisa@163.com (H.L.)

\* Correspondence: wuwei@ccucm.edu.cn; Tel.: +86-0431-86763991

**Abstract:** Polysaccharides are the main nutritional constituents in the *Armillaria mellea* fruiting bodies. The structure and immunoactivity of *Armillaria mellea* polysaccharide are valuable to be determined for development. In the present study, two polysaccharides, including *Armillaria mellea* neutral polysaccharide (AMPN) and *Armillaria mellea* acidic polysaccharide (AMPA), were prepared and determined. AMPN and AMPA were separated and refined by the ion exchange column and gel chromatography column. Analysis of AMPN and AMPA revealed molecular weights of  $4.432 \times 10^3$  Da and  $7.323 \times 10^3$  Da. The monosaccharide composition analysis revealed that AMPN was mainly composed of 68.3% glucose, while AMPA consisted primarily of glucose, mannose, and galactose, accompanied by 8.9% galacturonic acid and 3% fucose. Then, infrared spectra analysis, Congo red staining, methylation, and NMR spectroscopy analysis were conducted as a means to clarify the structure of AMPN and AMPA. The NMR spectra demonstrated that the two polysaccharides included both  $\alpha$  and  $\beta$ -configuration glycosidic bonds. The Congo red experiment suggests that AMPN and AMPA all had obvious triple helix structures. The effects of AMPN and AMPA on immune repair ability were compared by immune deficiency mice. The activity experiment showed that AMPN and acidic polysaccharides extracted from the *Armillaria* fruiting body have biological immune activity. Among them, AMPA showed higher immune activity. These findings suggest that *Armillaria mellea* fruiting bodies may be used as a source of dietary supplements and functional products.

**Keywords:** *Armillaria mellea*; polysaccharide; structural analysis; immunoactivity



**Citation:** Li, Q.; Li, Y.; Niu, H.; Wang, E.; Jiao, L.; Li, H.; Wu, W. Structure Elucidation and Immunoactivity Study of *Armillaria mellea* Fruiting Body Polysaccharides. *Separations* **2024**, *11*, 3. <https://doi.org/10.3390/separations11010003>

Academic Editors: Aleksandra Mišan and Gavino Sanna

Received: 14 November 2023

Revised: 8 December 2023

Accepted: 18 December 2023

Published: 20 December 2023



**Copyright:** © 2023 by the authors. Licensee MDPI, Basel, Switzerland. This article is an open access article distributed under the terms and conditions of the Creative Commons Attribution (CC BY) license (<https://creativecommons.org/licenses/by/4.0/>).

## 1. Introduction

*Armillaria mellea* (Vahl) P. Kumm is an edible fungus of the Subphylum Basidiomycotina, Order Agaricales, Tricholomataceae, and it has a symbiotic association with the orchid saprophytic plant *Gastrodia elata* [1]. *Armillaria mellea* fruiting bodies is an edible and medicinal fungus that is highly regarded in the areas of Northeast Asia, North America, and Europe due to its delicious taste and strong flavor [2,3]. This species is abundant in bioactive compounds, including polysaccharides, triterpenoids [4], amino acids, proteins, fatty acids, sterols, minerals, and vitamins [5]. It is a healthy food rich in various nutrients. Based on its growth and development stage, *Armillaria mellea* can be categorized into mycelium, rhizomorph, and fruiting bodies [6]. The majority of domestic and international research has primarily focused on the assessment of mycelium and rhizomorph [7], leading to the creation of diverse products such as Naoxinshu Oral Liquids, Mihunjun Tablets, Yuntongding Capsules, and Yinmi Tablets [2]. The chemical composition of *Armillaria mellea* has significant potential for application in medicine and functional foods. As a result, researchers have redirected their attention towards *Armillaria mellea* fruiting bodies, which possess a higher value [8,9]. Still, there is an absence of study on the composition and function of *Armillaria mellea* fruiting body polysaccharides. Concurrently, *Armillaria mellea*

is rich in polysaccharides and is considered a highly nutritious, low-fat food that should be consumed regularly [10]. Consequently, it is imperative to conduct further investigations into the *Armillaria mellea* polysaccharides (AMP) extracted from *Armillaria mellea* fruiting bodies. Polysaccharides, which are natural macromolecules manufactured up of more than ten monosaccharides together by glycoside chainbinding, are highly prevalent in edible mushrooms [8]. Various polysaccharide derivatives derived from renowned mushroom species, such as *Ganoderma lucidum* polysaccharides, *Coriolus* polysaccharides of *Trametes versicolor*, and *Lentinus edodes* polysaccharides, have been employed as medicinal agents or dietary supplements [11]. Compared with traditional drugs, polysaccharide-extracted fungi may be safer, have no toxic side effects, and could be used as supplements for functional foods [12,13].

The AMP is also the main nutrient component in *Armillaria mellea*, and it is a heteropolysaccharide mainly containing galactose, glucuronic acid, mannose, xylose, galacturonic acid, and arabinose with small amounts of other monosaccharides [14]. AMP has been proven to have activities of antioxidant [2,15], immune-enhancing [16], antidepressant [17], insomnia modulation [18,19], antiapoptotic [20], hypolipidemic, and hypoglycemic [21,22]. A study showed that AMP could promote splenocyte lymphocytes and macrophage proliferation, exhibiting significant immunomodulatory activities [23].

The extraction and purification methods have a significant impact on the preparation processes of polysaccharides. Different extraction methods, such as extraction solvent and temperature, will make the obtained polysaccharides show differences regarding structure and activity [24]. Water extraction, enzyme extraction, and ultrasonic-aided extraction are the three primary AMP extraction techniques that have been extensively studied [25]. Studies on the combined extraction of polysaccharides by different extraction methods have also been reported [21]. Hot water reflux extraction is a conventional technique for extracting polysaccharides. It offers the advantages of easy operation and the ability to retain water-soluble polysaccharides [26].

The crude polysaccharide extracted from *Armillaria mellea* contains protein and other impurities. While removing proteins and impurities, it also achieved the purpose of purifying polysaccharide components [27]. The two popular techniques for protein removal include the Sevag method [15,28] and the freeze–thaw method [29]. The crude polysaccharides obtained after the above separation and treatment still need to be further purified. Gel filtration chromatography and ion exchange chromatography are widely applied in the classification and purification of polysaccharides [30]. Gel filtration chromatography usually purifies several high-content polysaccharides from complex polysaccharide extracts based on their molecular weight. Derived from the properties of polysaccharides, ion exchange chromatography can achieve the segregation of neutral and acidic polysaccharides by gradient elution. The polysaccharides obtained by purifying polysaccharides with different gel chromatography, different types, and different concentrations of eluents are also different, mainly reflected in the molecular weight of polysaccharides, monosaccharide content, and other physical and chemical properties and structures.

The polysaccharides obtained using various extraction methods, separation, and purification methods have different monosaccharide composition ratios, monosaccharide sequences, glycosidic bonds, and polysaccharide configurations [31]. More polysaccharides with smaller molecular weights can be obtained by ultrasonic extraction [32]. These polysaccharides with different structures also showed different biological activities. Compared with ultrasonic-assisted extraction, the polysaccharides acquired during aqueous extraction have stronger activity in scavenging hydroxyl radicals [24]. The molecular weight of most polysaccharides with anti-inflammatory activity was between 6.9~192 kDa [14]. The  $\beta$ -1,6-Glc chain is a common structure with anti-tumor and immune activity in edible and medicinal fungus polysaccharides [6,33]. The  $\beta$ -1,6-Glc could accelerate the trend of polarization in M1 macrophages [34]. The polysaccharide containing  $\alpha$ -1,3-Gal and  $\alpha$ -Fuc structures was also confirmed to suppress the release of TNF- $\alpha$ . The  $\alpha$ -1,4-Glc and  $\alpha$ -1,4,6-Gal structures possess an effect on promoting lymphocyte proliferation [35,36]. Different

types and proportions of monosaccharide composition and structure make polysaccharides exhibit different biological activities. Therefore, we can regard *Armillaria mellea* as a dietary supplement and explore the structural characteristics of its role in enhancing immunity. The structural analysis of AMP mainly includes molecular weight determination, monosaccharide composition study, and glycosidic bond connection confirmation.

In this study, two polysaccharides, AMPN and AMPA, with different monosaccharide compositions, were extracted from *Armillaria mellea* fruiting bodies. The crude polysaccharide extracted from *Armillaria mellea* was isolated and refined through the DEAE-52 column and Sepharose gel chromatography. Meanwhile, the differences in the physicochemical properties of AMPN and AMPA were further analyzed and studied by IR spectra, GC-MS, and NMR spectra. Additionally, the immunomodulatory activities of AMPN and AMPA in immunosuppressed mice were conducted to lay the groundwork for the advancement of *Armillaria mellea* polysaccharides for use as healthy food.

## 2. Materials and Methods

### 2.1. Materials

*Amillariellmellea* fruiting bodies (crushed to about 0.25 mm pore size) were acquired from Antu Xinyu Edible and Medicinal Fungus Research and Development Co., Ltd. (Yanbian, China). 1-Phenyl-3-methyl-5-pyrazolone (PMP), DEAE-52 cellulose column, standard monosaccharides, trifluoroacetate (TFA), cellulase, papain, and Sepharose CL-6B gel chromatography were acquired from Yuanye Biotechnology Co., Ltd. (Shanghai, China). ELISA kits were acquired from Huangshi Yanke Co., Ltd. (Huangshi, Hubei, China). Other reagents were of analytical grade.

### 2.2. Preparation of AMPN and AMPA

Fruiting bodies of *Amillariellmellea* (500g) were weighed and then immersed in 10 L distilled water overnight. The sample was extracted twice with 100 °C hot water each for 4 h and filtered with a 300-mesh nylon cloth. Then, the *Amillariellmellea* polysaccharide (AMP) crude extract was merged and condensed under reduced pressure. After adding four times the volume of ethanol (95%), the residue was collected and composed to settle at 4 °C overnight. After centrifugation at 4000 rpm for 15 min, the precipitates underwent freeze-drying and were subsequently redissolved in water (*w/v*, 1:20) [27]. The sample-to-papain-to-cellulase ratio was set at 250:2:1, and the mixture was incubated at 45 °C for 2 h, followed by boiling for 15 min at 100 °C [37]. The crude extract of *Amillariellmellea* fruiting body polysaccharides was obtained by collecting the centrifugal supernatant and lyophilizing it.

### 2.3. Separation and Purification of AMPN and AMPA

The crude *Amillariellmellea* fruiting body polysaccharide was dissolved and subsequently placed onto the DEAE-52 cellulose column for elution with water and 1 M NaCl. Then, these two components obtained by different eluents were collected and separated through the Sepharose CL-6B column, which obtained the *Amillariellmellea* neutral polysaccharide (AMPN) and *Amillariellmellea* acidic polysaccharide (AMPA).

### 2.4. Determination of Physicochemical Properties and Structure

#### 2.4.1. Chemical Composition

The polysaccharide eluates were measured using a phenol-sulfuric acid assay to determine purity [38]. The protein content had been evaluated utilizing Bradford's methodology [39].

#### 2.4.2. Molecular Weight and Homogeneity

The molecular weights of AMPN and AMPA were analyzed using HPGPC. The standard curve was calibrated dependent on the dextran standard (T-180, 5250, 9750, 13,050, 36,800, 645,650, 135,350, and 300,600 Da). The UniMate™ 3000 HPLC system was used,

and the column temperature of the liquid phase system was 40 °C, the injection volume was 20 µL, and the mobile phase was ultrapure water in 0.5 mL·min<sup>-1</sup> [40].

#### 2.4.3. Monosaccharide Composition

Two polysaccharide samples (AMPN and AMPA) were initially hydrolyzed with 0.5 mL 2 M TFA, and this process lasted for 4 h under 120 °C. The dried hydrolysate was derivatized with PMP solvent and then extracted using chloroform. After drying, the hydrolysate was derivatized with PMP, and the resulting solution was then extracted using chloroform and repeated three times [23]. The purpose is to remove excessive PMP reagents. The aqueous phase was detected utilizing the Dionex™ UniMate™ 3000 HPLC system (Thermo Fisher Scientific, Waltham, MA, USA). The parameters of the HPLC were as follows: 40 °C for the column temperature, 250 nm for the detection wavelength, injection volume, 10 µL, mobile phase, acetonitrile (A, 15%), 0.1 M phosphate (pH 7.0, 85%) (B), flow rate, 0.8 mL·min<sup>-1</sup>.

#### 2.4.4. FTIR Analysis

Infrared spectra (IR) had been studied employing an FTIR spectrometer (Vector 33 spectrometer, Bruker, Germany). The polysaccharide samples were dried, mixed with KBr (1:100), and measured at 4000–500 cm<sup>-1</sup> [41].

#### 2.4.5. Methylation Analysis

Methylation analysis was performed on native polysaccharides that did not contain uronic acid polysaccharides or reduced polysaccharides [42,43]. The polysaccharide samples were analyzed by GC–MS (Thermo Fisher Scientific, USA) using dichloromethane as the solvent.

#### 2.4.6. NMR Spectroscopy Analysis

AMPN and AMPA were fully dissolved in 0.5 mL D<sub>2</sub>O solvent as test samples, and the 1D NMR spectra were recorded for the test samples on a Bruker-600FT-NMR spectrometer (Rheinstetten, Germany), including <sup>1</sup>H NMR and <sup>13</sup>C NMR.

#### 2.4.7. Congo Red Experiment

The conformational structures of AMPN and AMPA were determined by a Congo red assay according to the method described previously [44]. Congo red solution was blended with the AMPN and AMPA, respectively. Then 0.1, 0.2, 0.3, 0.4, 0.5, 0.6, 0.7, and 0.8 M NaOH solutions were added, and the mixture was agitated thoroughly. The ultraviolet (UV) range between 400 and 600 nm was chosen to measure the peak performance absorption wavelength.

### 2.5. Immune Activities of Polysaccharides

#### 2.5.1. Animals and Experimental Design

40 male Kunming mice (18–22 g, 4–5 weeks old) were bought from the Experimental Animal Center, Jilin University (Changchun, China), permission code SCXK 2021–0002. All animals were kept in strict accordance with the PR China legislation on the use and care of laboratory animals, the guidelines issued by the Experimental Animal Center of Changchun University of Chinese Medicine, and ratification by the University Animal Experimentation Committee. The mice were housed in separate cages, free to eat and drink water, at room temperature 22–25 °C, relative humidity 40–60%, in a light-dark environment with a 12-hour cycle. Before the experiment, the mice could adapt to the environment and diet for 7 days. The experimental mice were randomly divided into four groups (10 mice in each group), named control group (NC), model group (MC), AMPN group, and AMPA group. The mice in the NC and MC groups were given normal saline (0.1 mL·g<sup>-1</sup>·d<sup>-1</sup>) by gavage as a control, and the AMP-treated groups received AMPN and AMPA by gavage (200 mg·kg<sup>-1</sup>) for 21 days. With the sole instance of injecting normal

saline intraperitoneally toward the NC group as a control, intraperitoneal injection of CTX ( $80 \text{ mg}\cdot\text{kg}^{-1}\cdot\text{d}^{-1}$ ) established the immunodeficiency model on the 15th, 17th, 19th, and 21st days in the other groups. The orbital blood was collected and centrifuged (4000rpm, 15 min) from the mice to draw the serum. Following dissection, the thymuses, spleens, and colons of mice were removed and soaked in paraformaldehyde.

Based on the previous pre-experiment, three drug concentrations were explored, which were 50, 100, and  $200 \text{ mg}\cdot\text{kg}^{-1}$ . After a statistical analysis of the mice's body weight and immune-related index, it was concluded that the best immune effect of AMP in mice is  $200 \text{ mg}\cdot\text{kg}^{-1}$ , and the recovery degree of the mice's immune activity was proportional to the dose of AMP in a certain dose range. Therefore, the experimental method compares the immune activity of AMP in the high-dose group and analyzes the differences.

#### 2.5.2. Effect of the AMPN and AMPA on the Weight of Immune Organs

The mice's weight in the thymus and spleen was statistically counted, and the changed immune organ index was computed. The index of the thymus and spleen was articulated as the proportion of organ weight to body weight of mice ( $\text{mg}\cdot\text{g}^{-1}$ ) [45].

$$\text{Organ index (\%)} = \text{organ weight (mg)} / \text{body weight (g)} \times 100\%$$

#### 2.5.3. Determination of Blood Cell Count

The orbital blood had been extracted and processed by centrifugation to separate the plasma. The plasma was placed in an anticoagulant tube for the determination of white blood cells (WBC), platelets (PLT), red blood cells (RBC), lymphocytes (LYM), and neutrophils (NEU) [46].

#### 2.5.4. Determination of Cytokines

ELISA kits were used for determining the alterations of indicators (IL-2, IL-6, IgM, and IgA) in the serum of mice, and the corresponding instructions were followed [47].

#### 2.5.5. Colon Histopathological Examination

The colon ( $2 \times 2 \times 2 \text{ cm}$ ) of the dissected mice was fixed with a 4% formalin solution, buried in paraffin, sliced, and stained with hematoxylin–eosin (H&E). The histopathologic alterations of colon tissue were pointed out under the microscope [15].

### 2.6. Statistical Analysis

The one-way analysis of variance (ANOVA) was carried out using SPSS 21.0 statistical software. The data were expressed as mean  $\pm$  standard deviation (mean  $\pm$  SD), and  $p < 0.05$  was considered a difference with statistical significance.

## 3. Results and Discussion

### 3.1. Analysis of Physicochemical Properties and Structure

#### 3.1.1. Chemical Composition Analysis of AMPN and AMPA

*Amillariellmellea* neutral polysaccharide (AMPN) and *Amillariell mellea* acidic polysaccharide (AMPA) were acquired by water extraction and ethanol precipitation. Subsequently, the sample was eluted and separated by a DEAE column and Sepharose CL-6B chromatography. HPLC spectra and IR spectra of AMPN and AMPA were showed in Figure 1a–d. The two polysaccharide parts all showed a single peak in the HPLC spectrum, indicating that two homogeneous polysaccharide components were gained (Figure 1a,b). The purity of AMPN (47.21%) and AMPA (57.93%) was accepted by the phenol–sulfuric acid method (Table 1).

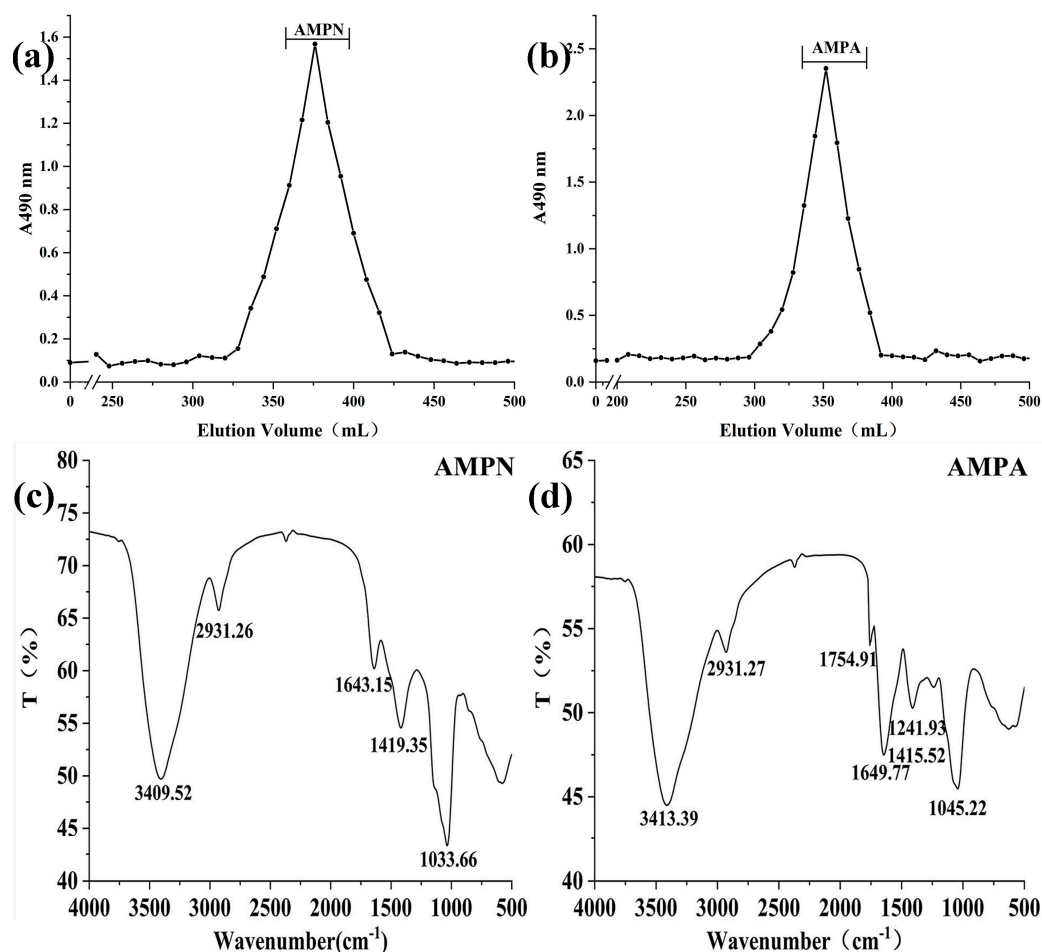


Figure 1. Sepharose CL-6B preparative chromatography of AMPN (a) and AMPA (b). IR spectra (4000–500 cm<sup>-1</sup>) of AMPN (c) and AMPA (d).

Table 1. Chemical characterization of the AMPN and AMPA.

Group	Total Sugar (%)	Protein (%)	Monosaccharide Composition (mol%)					
			Man	Glc	Ara	Gal	GlcA	Fuc
<i>Armillaria mellea</i> neutral polysaccharide (AMPN)	47.21	0.11	16.6	68.3	2.4	12.7	-	-
<i>Armillaria mellea</i> acidic polysaccharide (AMPA)	57.93	0.17	26.9	31.3	7.5	22.4	8.9	3

“-”: not detected.

### 3.1.2. Molecular Weight Detection

The HPGPC method was used to ascertain the molecular weights of AMPA and AMPN. The standard curve was established to calculate the average molecular weight (Mw). The equation of the standard curve was:  $\log Mw = -0.3085t + 10.147$ ,  $R^2 = 0.9937$ . The elution time of AMPN and AMPA was 27.071 min and 20.364 min. The average molecular weights of AMPN and AMPA were  $4.432 \times 10^3$  Da and  $7.323 \times 10^3$  Da, respectively.

### 3.1.3. Monosaccharide Composition

Figure 2a–d showed HPLC elution profiles of monosaccharide composition, derived monosaccharide standards, and the Congo red experiment changes in absorption maximum. The AMPN and AMPA monosaccharide content was detected, and the retention time was determined by standard monosaccharide derivatives (Figure 2a–c). The peak area of monosaccharides was integrated, and the ratio of peak area to standard was determined.

Finally, the molar ratio of monosaccharides was determined by normalization [12,47]. The investigation of monosaccharide content (Table 1) specified that AMPN was mainly composed of glucose (68.3%) without uronic acid. AMPA was an acid heteropolysaccharide dominated by glucose, mannose, and galactose, with glucuronic acid (8.9%). These findings showed that glucose was the predominant monosaccharide in AMPN, while glucose, mannose, and galactose were the predominant monosaccharides in AMPA.

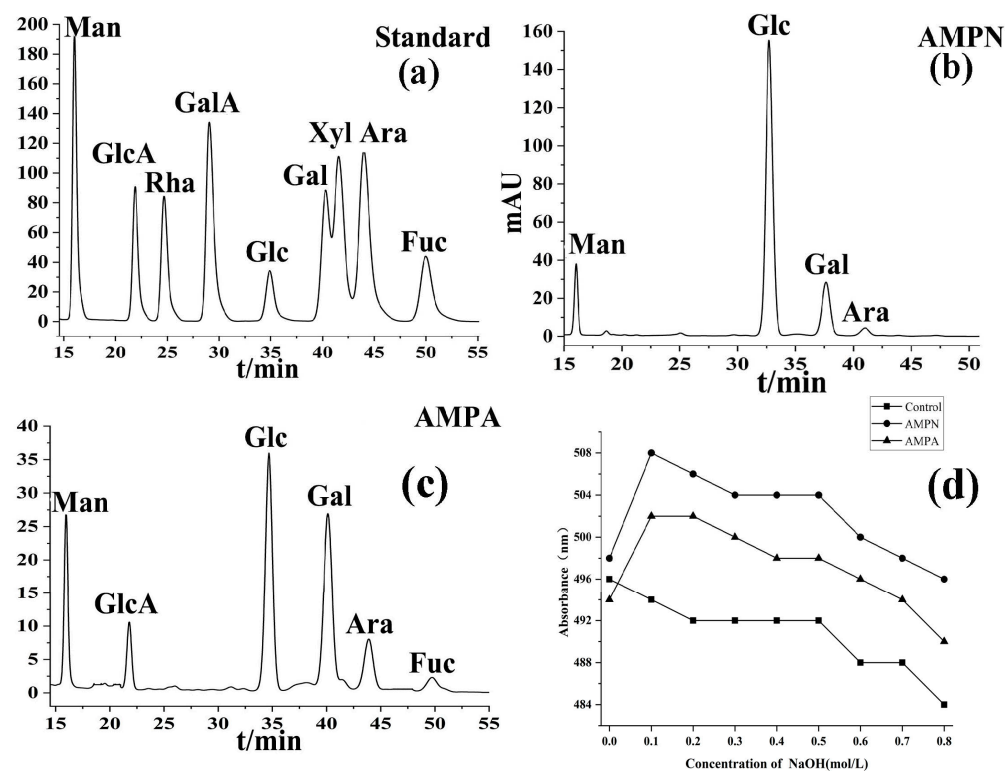


**Figure 2.** HPLC elution profiles of monosaccharide composition, derived monosaccharide standards (a), AMPN (b), AMPA(c), and the Congo red experiment changes in absorption maximum (d).

### 3.1.4. IR Spectra Analysis

When determining the functional structure of polysaccharides, IR spectra are a common and reliable method, with wave numbers ranging from  $4000\text{--}500\text{ cm}^{-1}$  (Figure 1c,d). The absorption peaks located at  $3409.52\text{ cm}^{-1}$  and  $3413.39\text{ cm}^{-1}$  are broad and strong, which are the characteristic absorption of the O–H bond. The signal at  $2931.26\text{ cm}^{-1}$  was assigned to the C–H stretching vibration absorption of polysaccharides. The absorption signal located at  $1754.91\text{ cm}^{-1}$  that was observed in AMPA was attributed to the carboxyl groups, indicating that AMPA contains uronic acid. The signals at  $1419.35\text{ cm}^{-1}$  and  $1415.52\text{ cm}^{-1}$  are united by C=C bonds. In addition, the appearance of the signal at  $1241.93\text{ cm}^{-1}$  means that the polysaccharide structure has the characteristic signal of C–O–H on the pyran ring, and the absorption signals at  $1033.66\text{ cm}^{-1}$  and  $1045.22\text{ cm}^{-1}$  are related to the stretching vibration of C=O on the pyran ring [30]. The findings suggest that AMPA and AMPN may contain a pyran ring structure.

### 3.1.5. Methylation Analysis

Methylation has been utilized to investigate the structure of polysaccharides. Because the presence of Glc A will make the values of Glc and Glc A in the methylation analysis results inaccurate, AMPA first carried out the reduction reaction of uronic acid, followed by the methylation reaction. The methylation results and the glycosidic bond connection of AMPN and AMPA-R are shown in Table 2. The finding indicated that 1,2,4-linked glucosyl (62.0%) was the most abundant component in AMPN; the 1,2,4-linked glucosyl (33.9%), 1-mannose (22.4%), and 1-galactosyl (26.7%) residues were mainly present in the backbone

structure of AMPA. This result verified the conclusion of the monosaccharide composition analysis:Glc content is the majority in the AMPN, while AMPA is dominated by Glc, Man, and Gal.

**Table 2.** Methylation results of AMPN and AMPA.

Methylated Sugar	Type of Linkage	Molar (%)	
		AMPN	AMPA
2,3,4,6-Me <sub>4</sub> -Gal	Gal-(1→	3	26.7
2,3,4,6-Me <sub>4</sub> -Man	Man-(1→	16.2	22.4
2,3,4-Me <sub>3</sub> -Gal	→6)-Gal-(1→	0.2	-
2,3,4-Me <sub>3</sub> -Man	→6)-Man-(1→	0.3	-
2,3,5-Me <sub>3</sub> -Ara	Ara-(1→	1.4	1.1
2,3,6-Me <sub>3</sub> -Glc	→4)-Glc-(1→	6.2	-
2,3-Me <sub>2</sub> -Ara	→5)-Ara-(1→	1.1	4.7
2,4,6-Me <sub>3</sub> -Gal	→3)-Gal-(1→	7.9	-
3,6-Me <sub>2</sub> -Glc	→2,4)-Glc-(1→	62	33.9
3-Me-Fuc	→2,4)-Fuc-(1→	-	2.2
2,3,4-Me <sub>3</sub> -Fuc	Fuc-(1→	-	1.4
2,4,6-Me <sub>3</sub> -Man	→2)-Man-(1→	-	7.4

### 3.1.6. NMR Spectroscopy Analysis

The structures of AMPN and AMPA were further analyzed by NMR (Figure 3). Nearly all NMR proton signals manifested within the scope of <sup>1</sup>Hδ 4.5–5.5 ppm and <sup>13</sup>Cδ 90–108 ppm, which is a typical distribution of polysaccharides in NMR signals. In the <sup>1</sup>H protons region, the signals δ 4.3–3.0 ppm belong to the signal generated by the ring protons of carbons on the glycosidic ring, signifying the skeleton has glycosidic bonds [48]. The anomeric protons with a chemical shift higher than δ5.0 are generally resonance signals of polysaccharide residues with α-glycosidic bonds, while small δ5.0 is a β-glycosidic bond commonly. The chemical shift in <sup>13</sup>C NMR of the α-configuration is δ92–100 ppm, and the <sup>13</sup>C NMR signal of the β-configuration is δ100–108 ppm [49,50]. The strong signal in <sup>1</sup>H at 4.69 ppm was the response of the residual solvent (D2O). The glycosidic bond was positioned according to the previously reported literature and methylation results; →2,4)-α-Glc(1→ was assigned to the signals at δ 5.32/98.59 [36]. Chemical shifts of δ 5.32, 5.22, 5.16, 5.12, and 5.08 ppm in <sup>1</sup>H and δ 108.23, 107.51, 104.19, 102.3, 98.59, 97.96, and 96.01 in <sup>13</sup>C indicate two polysaccharides all had α and β glycoside bonds. There was no signal peak at 82–88 ppm in the <sup>13</sup>C NMR spectrum, verifying that both polysaccharide residues were pyranose [51]. Meanwhile, the signals at 175.07 ppm (in AMPA) belong to the C-6 characteristic absorption peak of uronic acid, which verifies that AMPA is an acidic polysaccharide. The results of NMR determined the regions of proton hydrogen and anomeric carbon of the two polysaccharides. It can be concluded that both AMPA and AMPN are pyran-type polysaccharides containing α and β anomeric configurations of glycosidic bonds [36,52]. Due to the high overlap of the correlation between H-1 and H-2/3/4/6, it was hard to distinguish the remaining monosaccharide structures. Therefore, further exploration of its deep structure needs to be judged by 2D-NMR.

### 3.1.7. Congo Red Analysis of AMPN and AMPA

The changes in the Congo red experiment's absorption maximum are shown in Figure 2d. Congo red is a jujube red acid dye. Congo red is often combined with polysaccharides, which have a triple helix conformation, to form complexes. With the addition of NaOH solution, the complex formed by Congo red and polysaccharide gradually disappears, illustrating the red shift in the maximum absorption wavelength. In a certain concentration range, it can be inferred whether the AMPN and AMPA have a helical conformation by the changing trend of the wavelength [31,53]. The UV spectrum maximum absorption wavelength started to decrease after NaOH approached 0.1 M (Figure 2d), suggesting the presence of a three-stranded spiral conformation in AMPN and AMPA.

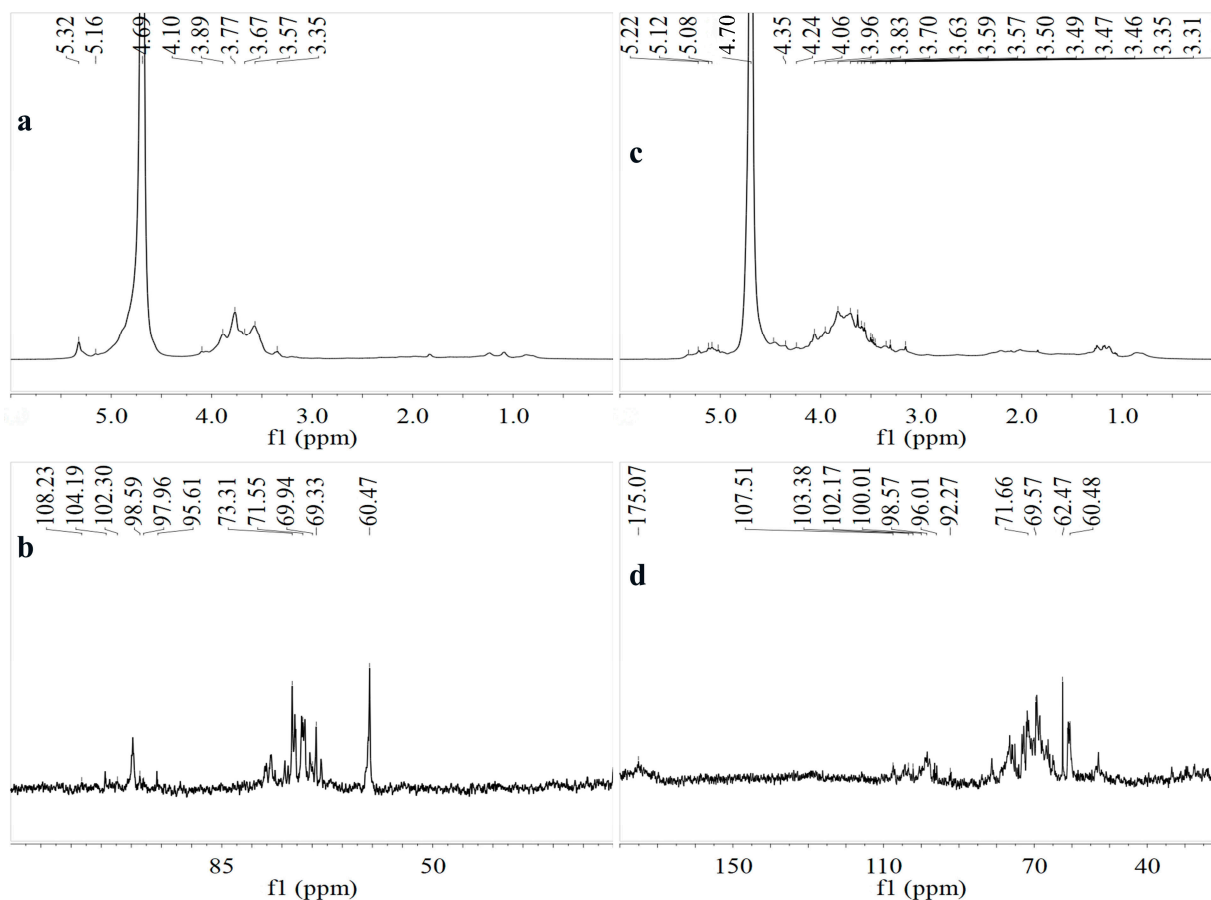


**Figure 3.** The results of the NMR spectrum analysis. <sup>1</sup>H NMR spectra of AMPN (a), <sup>13</sup>C NMR spectra of AMPN (b), <sup>1</sup>H NMR spectra of AMPA (c), and <sup>13</sup>C NMR spectra of AMPA (d).

### 3.2. Effects of AMPN and AMPA in Immunosuppressive Mice

#### 3.2.1. Effects of the AMPN and AMPA on Body Weight

Cyclophosphamide is a potent immune suppressant that causes CTX-induced damage to the body’s normal cells, leading to biological weight loss [45]. Figure 4a,b showed the effects of AMPN and AMPN on body weight and the secretion of immune organ index. The mouse body weight variation trend showed an upward trend among all groups in the first 15 days (Figure 4a). The weight development velocity during the same period was propinquity in each group. On the 15th day, the MC group and the administration groups were injected with CTX every other day. The body weight of mice in the AMPN, AMPA, and MC groups decreased significantly due to the injection of cyclophosphamide, while the weight in the NC group continued to increase. The mice showed emaciation, withered hair, curled up, slow response, low food intake, and timidity. In the comparison of the three CTX injection groups of AMPN, AMPA, and MC, the AMPN and AMPA administration groups significantly alleviated the weight loss of mice. It demonstrates that AMPN and AMPA may lead mice to gain additional body weight by resisting the side effects of CTX.

#### 3.2.2. Effects of the AMPN and AMPN on Immune Organ Index

The thymus and spleen are vital immunological organs in organisms. Immune cells undergo development and multiplication in these two locations. The thymus is the central immune organ that mainly mediates cellular immunity, and the spleen is a secondary immune organ involved in humoral immunity [54]. The thymus and spleen index, which is a crucial indicator for assessing the immunological function of organs, can show the growth and development of the thymus and spleen [55]. Meanwhile, research has demonstrated that polysaccharides can significantly increase spleen cell proliferation [48,56,57], which

is the same as the data obtained in this study (Figure 4b). Compared with the NC group, the immune organ levels of the MC group were significantly lower, which shows that cyclophosphamide caused damage to the mice’s immune system [58]. The AMPN and AMPA groups were able to promote higher thymus and spleen indexes in comparison to the MC group. The AMPN treatment group’s spleen and thymus indexes increased by 35.1% and 18.8%, respectively. The AMPA treatment group’s spleen and thymus indexes increased by 33.0% and 21.5%, respectively. Based on the decreased or increased immune organ index, we may conclude that AMPN and AMPA may play an immunoregulatory role by repairing damaged immune organs to restore the function of immune organs.

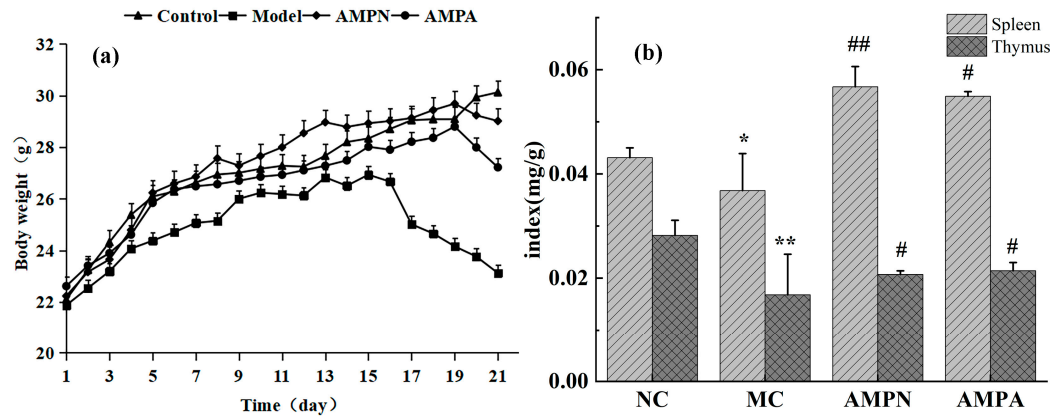


**Figure 4.** Effects of AMPN and AMPN on body weight (a) and the secretion of immune organ index (b). The data are expressed as mean ± SD. \* comparison with NC group, \*  $p < 0.05$ , \*\*  $p < 0.01$ . # comparison with the MC group, #  $p < 0.05$ , ##  $p < 0.01$ .

### 3.2.3. Effect of AMPN and AMPN on Clinical Biochemical Parameters

The immune system is an important physiological function. It is a multifunctional defense system that protects the host from pathogenic microorganisms or damaged cells produced in the body by monitoring and identifying its own and nonself components to maintain health. We evaluated the levels of white blood cells (WBCs), lymphocytes (LYMs), red blood cells (RBCs), neutrophils (NEUs), and platelets (PLTs) in the mouse blood cell count experiment (Figure 5a–e). Compared with the NC group, due to the injection of CTX, the number of immune cells in the MC group significantly decreased. Compared with the MC group, the cell indicators of the AMPN and AMPA administration were significantly restored. The indicators of WBC, RBC, LYM, PLT, and NEU in the AMPN treatment group increased by 27.8%, 4.3%, 49.3%, 28.2%, and 23.3%, and the AMPA treatment group increased by 41.9%, 9.9%, 53.1%, 28.2%, and 61.8%. AMPN played a stronger role in promoting the growth of immune cell indexes in mice. It was discovered that AMPN and AMPA had the function of preventing CTX from damaging lymphocytes.

An ELISA kit was used to detect the concentration changes of immunoglobulin IgM, IgA, IL-2, and IL-6 (Figure 5f–i). The concentration of antibodies in the MC group was markedly lower compared to the NC group. Under the action of AMPN and AMPA, the concentrations of immunoglobulin in the AMPN group were significantly increased by 2.3%, 6.9%, 6.5%, and 4.8%, whereas the degrees of immune antibody in the AMPA treatment group were increased by 9.7%, 9.0%, 6.4%, and 8.4%. In conclusion, AMPN and AMPA could significantly promote the production of cytokines, which indicates that AMP could enhance immunocompetence.

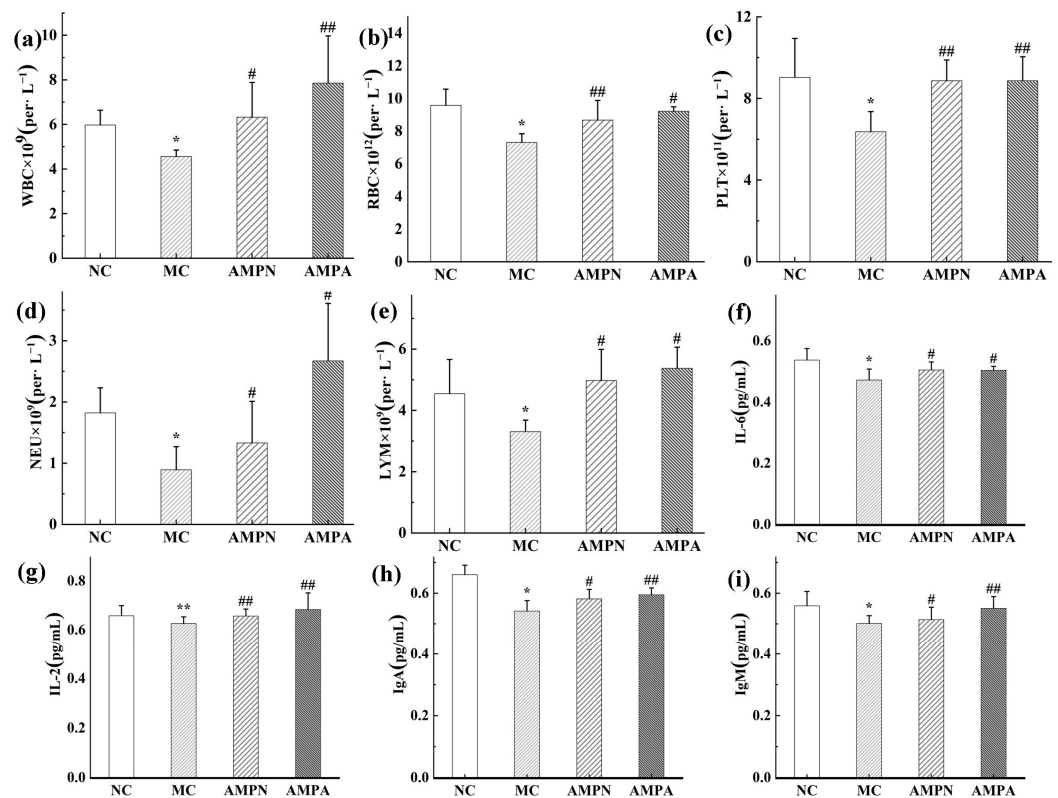


**Figure 5.** The levels of WBC (a), RBC (b), LYM (c), PLT (d), NEU (e), IgM (f), IgA (g), IL-2 (h), and IL-6 (i) in the blood cell count. The data are expressed as the mean ± SD. \* comparison with NC group, \*  $p < 0.05$ , \*\*  $p < 0.01$ . # comparison with MC group, #  $p < 0.05$ , ##  $p < 0.01$ .

### 3.2.4. Effects of AMP on Colon Tissue

The integrity of intestinal morphology determines whether the intestinal barrier function can function normally [59,60]. The crypt depth and villus height serve as markers for assessing the intestinal morphology's integrity [61,62]. In general, the longer intestinal villus and the deeper crypt represent the intestinal tract in a better state; the structure and function are normal, and the intestinal tract can play a normal immune role [63]. The impact of AMPN and AMPA on the internal morphology of colon tissue in mice was observed after H&E staining of colon tissue (Figure 6). The NC group of the mice morphological structure of intestinal villus distributed on the intestinal surface was normal. Compared with the NC group, the crypt depth and villus height decreased after the injection of CTX. Additionally, mucosal epithelial cell degeneration, loose cytoplasmic light staining, and sparsely arranged intestinal glands in the lamina propria were observed. Compared with the mice's colonic tissue that was observed in the MC group, the morphology recovery of the AMPN and AMPA groups was better. These indicate that AMPN and AMPA can improve the damage to intestinal mucosal cells.

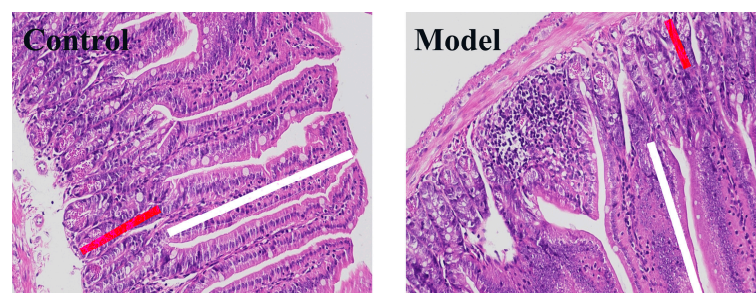


**Figure 6.** Cont.

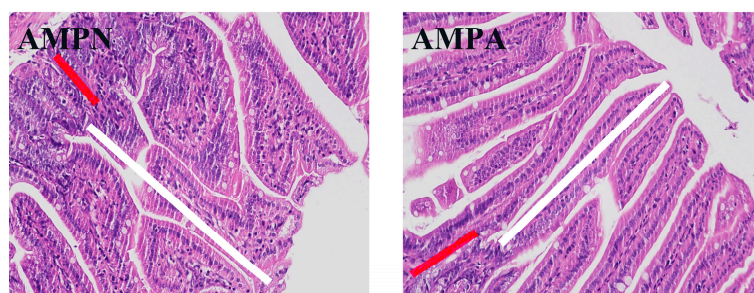


**Figure 6.** Colon tissue with H&E staining (magnification 400 $\times$ , scale bars 20  $\mu$ m). The white line segment represents the villus length and the red line segment shows the crypt depth.

#### 4. Conclusions

Two novel water-soluble polysaccharides were isolated from the fruiting bodies of *Armillaria mellea* by DEAE-52 ion exchange column and gel chromatography, and their structures were identified. Analyses of chemical composition and structure revealed that AMPN had a molecular weight of  $4.432 \times 10^3$  Da and AMPA had a molecular weight of  $7.323 \times 10^3$  Da. AMPN was made up of mannose, arabinose, galactose, and glucose. AMPA is made up of galacturonic acid, fucose, glucose, mannose, arabinose and galactose. Meanwhile, the results obtained from the experiment show that both AMPN and AMPA are pyranoses containing  $\alpha$  and  $\beta$  configuration glycosidic bonds, and it is judged that both polysaccharides have a triple helix structure. Among them, AMPA has a richer monosaccharide composition and shows more proton signals in  $^{13}\text{C}$  NMR. In the study of immune activity, we found that AMPN and AMPA can alleviate weight loss and immune organ atrophy caused by immunosuppressive mouse models. Notably, AMPA exhibited more effective resistance to the effect of CTX-induced immunosuppression and recovery of immune organ index than AMPN, indicating that the former showed more effective potential for immunomodulator applications. Overall, AMP has the potential for immunomodulatory activity, which warrants further research.

**Author Contributions:** Conceptualization, Q.-Q.L. and W.W.; methodology, E.-H.W. and W.W.; software, Y.L. and H.-Z.N.; validation, W.W.; investigation, Q.-Q.L., H.L. and L.-L.J.; data curation, Y.L. and H.-Z.N.; writing—original draft preparation, E.-H.W. and Q.-Q.L.; writing—review and editing, W.W.; supervision, W.W.; funding acquisition, W.W. All authors have read and agreed to the published version of the manuscript.

**Funding:** This research was funded by the Science and Technology Development Plan Project of Jilin Province (20200708042YY).

**Institutional Review Board Statement:** This study was conducted following the Declaration of Helsinki and approved by the Institutional Animal Care and Use Committee (IACUC) of the Changchun University of Chinese Medicine (protocol CPCUCM IACUC 2020246-1 on 17 September 2020).

**Data Availability Statement:** All the data used in this study are available within this article. Further inquiries can be directed to the authors.

**Conflicts of Interest:** All the authors declare that they have no conflict of interest.

#### References

1. Lin, Y.-E.; Wang, H.-L.; Lu, K.-H.; Huang, Y.-J.; Panyod, S.; Liu, W.-T.; Yang, S.-H.; Chen, M.-H.; Lu, Y.-S.; Sheen, L.-Y. Water extract of *Armillaria mellea* (Vahl) P. Kumm. Alleviates the depression-like behaviors in acute- and chronic mild stress-induced rodent models via anti-inflammatory action. *J. Ethnopharmacol.* **2021**, *265*, 113395. [[CrossRef](#)]
2. Zhang, S.; Liu, X.; Yan, L.; Zhang, Q.; Zhu, J.; Huang, N.; Wang, Z. Chemical compositions and antioxidant activities of polysaccharides from the sporophores and cultured products of *Armillaria mellea*. *Molecules* **2015**, *20*, 5680–5697. [[CrossRef](#)]
3. Štrapáč, I.; Baranová, M.; Smrčová, M.; Bedlovičová, Z. Antioxidant Activity of Honey Mushrooms (*Armillaria mellea*). *Folia Vet.* **2016**, *60*, 37–41. [[CrossRef](#)]
4. Dörfer, M.; Gressler, M.; Hoffmeister, D. Diversity and bioactivity of *Armillaria* sesquiterpene aryl ester natural products. *Mycol. Prog.* **2019**, *18*, 1027–1037. [[CrossRef](#)]

5. Huang, J.-W.; Lai, C.-J.-S.; Yuan, Y.; Zhang, M.; Zhou, J.-H.; Huang, L.-Q. Correlative analysis advance of chemical constituents of *Polyporusumbellatus* and *Armillaria mellea*. *Zhongguo Zhong Yao Za Zhi* **2017**, *42*, 2905–2914.
6. Muszyńska, B.; Sułkowska-Ziaja, K.; Wołkowska, M.; Ekiert, H. Chemical, pharmacological, and biological characterization of the culinary-medicinal honey mushroom, *Armillaria mellea* (Vahl) P. Kumm. (Agaricomycetidae): A review. *Int. J. Med. Mushrooms* **2011**, *13*, 167–175. [[CrossRef](#)]
7. Geng, Y.; Zhu, S.; Lu, Z.; Xu, H.; Shi, J.-S.; Xu, Z.-H. Anti-inflammatory activity of mycelial extracts from medicinal mushrooms. *Int. J. Med. Mushrooms* **2014**, *16*, 319–325. [[CrossRef](#)]
8. Ren, S.; Gao, Y.; Li, H.; Ma, H.; Han, X.; Yang, Z.; Chen, W. Research Status and Application Prospects of the Medicinal Mushroom *Armillaria mellea*. *Appl. Biochem. Biotechnol.* **2023**, *195*, 3491–3507. [[CrossRef](#)]
9. Nowacka-Jechalke, N.; Kanak, S.; Moczulski, M.; Martyna, A.; Kubiński, K.; Masłyk, M.; Szpakowska, N.; Kaczyński, Z.; Nowak, R.; Olech, M. Crude Polysaccharides from Wild-Growing *Armillaria mellea*—Chemical Composition and Antidiabetic, Anti-Inflammatory, Antioxidant, and Antiproliferative Potential. *Appl. Sci.* **2023**, *13*, 3853. [[CrossRef](#)]
10. Kostić, M.; Smiljković, M.; Petrović, J.; Glamočlija, J.; Barros, L.; Ferreira, I.C.F.R.; Ćirić, A.; Soković, M. Chemical, nutritive composition and a wide range of bioactive properties of honey mushroom *Armillaria mellea* (Vahl: Fr.) Kummer. *Food Funct.* **2017**, *8*, 3239–3249. [[CrossRef](#)]
11. Han, S.-S.R.; Cho, C.-K.; Lee, Y.-W.; Yoo, H.-S. Antimetastatic and immunomodulating effect of water extracts from various mushrooms. *J. Acupunct. Meridian Stud.* **2009**, *2*, 218–227. [[CrossRef](#)]
12. Wei, X.; Yao, J.; Wang, F.; Wu, D.; Zhang, R. Extraction, isolation, structural characterization, and antioxidant activity of polysaccharides from elderberry fruit. *Front. Nutr.* **2022**, *9*, 947706. [[CrossRef](#)]
13. Wu, J.; Zhou, J.; Lang, Y.; Yao, L.; Xu, H.; Shi, H.; Xu, S. A polysaccharide from *Armillaria mellea* exhibits strong in vitro anticancer activity via apoptosis-involved mechanisms. *Int. J. Biol. Macromol.* **2012**, *51*, 663–667. [[CrossRef](#)]
14. Guo, Y.; Chen, X.; Gong, P. Classification, structure and mechanism of antiviral polysaccharides derived from edible and medicinal fungus. *Int. J. Biol. Macromol.* **2021**, *183*, 1753–1773. [[CrossRef](#)]
15. Li, H.; Xu, G.; Yuan, G. Effects of an *Armillaria mellea* Polysaccharide on Learning and Memory of D-Galactose-Induced Aging Mice. *Front. Pharmacol.* **2022**, *13*, 919920. [[CrossRef](#)]
16. Yan, J.; Han, Z.; Qu, Y.; Yao, C.; Shen, D.; Tai, G.; Cheng, H.; Zhou, Y. Structure elucidation and immunomodulatory activity of a  $\beta$ -glucan derived from the fruiting bodies of *Armillariellamellea*. *Food Chem.* **2018**, *240*, 534–543. [[CrossRef](#)]
17. Zhang, T.; Du, Y.; Liu, X.; Sun, X.; Cai, E.; Zhu, H.; Zhao, Y. Study on antidepressant-like effect of protoilludane sesquiterpenoid aromatic esters from *Armillaria mellea*. *Nat. Prod. Res.* **2021**, *35*, 1042–1045. [[CrossRef](#)]
18. Yao, L.; Lv, J.; Duan, C.; An, X.; Zhang, C.; Li, D.; Li, C.; Liu, S. *Armillaria mellea* fermentation liquor ameliorates p-chlorophenylalanine-induced insomnia associated with the modulation of serotonergic system and gut microbiota in rats. *J. Food Biochem.* **2022**, *46*, e14075. [[CrossRef](#)]
19. Li, I.-C.; Lin, T.-W.; Lee, T.-Y.; Lo, Y.; Jiang, Y.-M.; Kuo, Y.-H.; Chen, C.-C.; Chang, F.-C. Oral Administration of *Armillaria mellea* Mycelia Promotes Non-Rapid Eye Movement and Rapid Eye Movement Sleep in Rats. *J. Fungi* **2021**, *7*, 371. [[CrossRef](#)]
20. An, S.; Lu, W.; Zhang, Y.; Yuan, Q.; Wang, D. Pharmacological Basis for Use of *Armillaria mellea* Polysaccharides in Alzheimer’s Disease: Antiapoptosis and Antioxidation. *Oxid. Med. Cell Longev.* **2017**, *2017*, 4184562. [[CrossRef](#)]
21. Li, X.; Zhu, J.; Wang, T.; Sun, J.; Guo, T.; Zhang, L.; Yu, G.; Xia, X. Antidiabetic activity of *Armillaria mellea* polysaccharides: Joint ultrasonic and enzyme assisted extraction. *Ultrason. Sonochem.* **2023**, *95*, 106370. [[CrossRef](#)]
22. Yang, S.; Yan, J.; Yang, L.; Meng, Y.; Wang, N.; He, C.; Fan, Y.; Zhou, Y. Alkali-soluble polysaccharides from mushroom fruiting bodies improve insulin resistance. *Int. J. Biol. Macromol.* **2019**, *126*, 466–474. [[CrossRef](#)]
23. Chen, R.; Ren, X.; Yin, W.; Lu, J.; Tian, L.; Zhao, L.; Yang, R.; Luo, S. Ultrasonic disruption extraction, characterization and bioactivities of polysaccharides from wild *Armillaria mellea*. *Int. J. Biol. Macromol.* **2020**, *156*, 1491–1502. [[CrossRef](#)]
24. Jing, Y.; Yan, M.; Zhang, H.; Liu, D.; Qiu, X.; Hu, B.; Zhang, D.; Zheng, Y.; Wu, L. Effects of Extraction Methods on the Physicochemical Properties and Biological Activities of Polysaccharides from *Polygonatum sibiricum*. *Foods* **2023**, *12*, 2088. [[CrossRef](#)]
25. Lung, M.-Y.; Chang, Y.-C. Antioxidant properties of the edible Basidiomycete *Armillaria mellea* in submerged cultures. *Int. J. Mol. Sci.* **2011**, *12*, 6367–6384. [[CrossRef](#)]
26. Latgé, J.-P. The cell wall: A carbohydrate armour for the fungal cell. *Mol. Microbiol.* **2007**, *66*, 279–290. [[CrossRef](#)]
27. Nai, J.; Zhang, C.; Shao, H.; Li, B.; Li, H.; Gao, L.; Dai, M.; Zhu, L.; Sheng, H. Extraction, structure, pharmacological activities and drug carrier applications of *Angelica sinensis* polysaccharide. *Int. J. Biol. Macromol.* **2021**, *183*, 2337–2353. [[CrossRef](#)]
28. Fu, J.; Li, J.; Sun, Y.; Liu, S.; Song, F.; Liu, Z. In-depth investigation of the mechanisms of *Schisandra chinensis* polysaccharide mitigating Alzheimer’s disease rat via gut microbiota and feces metabolomics. *Int. J. Biol. Macromol.* **2023**, *232*, 123488. [[CrossRef](#)]
29. Zhao, G.; Hou, X.; Li, X.; Qu, M.; Tong, C.; Li, W. Metabolomics analysis of alloxan-induced diabetes in mice using UPLC–Q-TOF-MS after *Crassostrea gigas* polysaccharide treatment. *Int. J. Biol. Macromol.* **2018**, *108*, 550–557. [[CrossRef](#)]
30. Molaei, H.; Jahanbin, K. Structural features of a new water-soluble polysaccharide from the gum exudates of *Amygdalus scoparia* Spach (*Zedo gum*). *Carbohydr. Polym.* **2018**, *182*, 98–105. [[CrossRef](#)]
31. Liu, Y.; Zhang, Y.; Mei, N.; Li, W.; Yang, T.; Xie, J. Three acidic polysaccharides derived from sour jujube seeds protect intestinal epithelial barrier function in LPS induced Caco-2 cell inflammation model. *Int. J. Biol. Macromol.* **2023**, *240*, 124435. [[CrossRef](#)] [[PubMed](#)]

32. Huang, X.; Zhang, Y.; Xie, N.; Cheng, J.; Wang, Y.; Yuan, S.; Li, Q.; Shi, R.; He, L.; Chen, M. Molecular Characterization and Bioactivities of a Novel Polysaccharide from *Phyllostachys praececox* Bamboo Shoot Residues. *Foods* **2023**, *12*, 1758. [[CrossRef](#)] [[PubMed](#)]
33. Siu, K.-C.; Xu, L.; Chen, X.; Wu, J.-Y. Molecular properties and antioxidant activities of polysaccharides isolated from alkaline extract of wild *Armillaria ostoyae* mushrooms. *Carbohydr. Polym.* **2016**, *137*, 739–746. [[CrossRef](#)] [[PubMed](#)]
34. Cheng, H.; Sun, L.; Shen, D.; Ren, A.; Ma, F.; Tai, G.; Fan, L.; Zhou, Y. Beta-1,6 glucan converts tumor-associated macrophages into an M1-like phenotype. *Carbohydr. Polym.* **2020**, *247*, 116715. [[CrossRef](#)] [[PubMed](#)]
35. Chang, C.-C.; Cheng, J.-J.; Lee, I.-J.; Lu, M.-K. Purification, structural elucidation, and anti-inflammatory activity of xylosylgalactofucan from *Armillaria mellea*. *Int. J. Biol. Macromol.* **2018**, *114*, 584–591. [[CrossRef](#)] [[PubMed](#)]
36. Li, B.; Zhang, N.; Feng, Q.; Li, H.; Wang, D.; Ma, L.; Liu, S.; Chen, C.; Wu, W.; Jiao, L. The core structure characterization and of ginseng neutral polysaccharide with the immune-enhancing activity. *Int. J. Biol. Macromol.* **2019**, *123*, 713–722. [[CrossRef](#)] [[PubMed](#)]
37. Sun, Y.; Liang, H.; Zhang, X.; Tong, H.; Liu, J. Structural elucidation and immunological activity of a polysaccharide from the fruiting body of *Armillaria mellea*. *Bioresour. Technol.* **2009**, *100*, 1860–1863. [[CrossRef](#)] [[PubMed](#)]
38. Masuko, T.; Minami, A.; Iwasaki, N.; Majima, T.; Nishimura, S.-I.; Lee, Y.C. Carbohydrate analysis by a phenol-sulfuric acid method in microplate format. *Anal. Biochem.* **2005**, *339*, 69–72. [[CrossRef](#)]
39. Kruger, N.J. The Bradford method for protein quantitation. *Methods Mol. Biol.* **1994**, *32*, 9–15.
40. Kumar, V.; Rana, V.; Soni, P.L. Molecular weight determination and correlation analysis of Dalbergia sissoo polysaccharide with constituent oligosaccharides. *Phytochem. Anal.* **2013**, *24*, 75–80. [[CrossRef](#)]
41. Yu, G.; Yue, C.; Zang, X.; Chen, C.; Dong, L.; Liu, Y. Purification, characterization and in vitro bile salt-binding capacity of polysaccharides from *Armillaria mellea* mushroom. *Czech J. Food Sci.* **2019**, *37*, 51–56. [[CrossRef](#)]
42. Jiao, L.; Li, H.; Li, J.; Bo, L.; Zhang, X.; Wu, W.; Chen, C. Study on structure characterization of pectin from the steamed ginseng and the inhibition activity of lipid accumulation in oleic acid-induced HepG2 cells. *Int. J. Biol. Macromol.* **2020**, *159*, 57–65. [[CrossRef](#)] [[PubMed](#)]
43. Fu, Y.-P.; Li, C.-Y.; Peng, X.; Zou, Y.-F.; Rise, F.; Paulsen, B.S.; Wangensteen, H.; Inngjerdingen, K.T. Polysaccharides from *Aconitum carmichaelii* leaves: Structure, immunomodulatory and anti-inflammatory activities. *Carbohydr. Polym.* **2022**, *291*, 119655. [[CrossRef](#)] [[PubMed](#)]
44. Zhang, X.; Zhang, X.; Gu, S.; Pan, L.; Sun, H.; Gong, E.; Zhu, Z.; Wen, T.; Daba, G.M.; Elkhateeb, W.A. Structure analysis and antioxidant activity of polysaccharide-iron (III) from *Cordyceps militaris* mycelia. *Int. J. Biol. Macromol.* **2021**, *178*, 170–179. [[CrossRef](#)] [[PubMed](#)]
45. Dai, J.; Chen, J.; Qi, J.; Ding, M.; Liu, W.; Shao, T.; Han, J.; Wang, G. Konjac Glucomannan from *Amorphophallus konjac* enhances immunocompetence of the cyclophosphamide-induced immunosuppressed mice. *Food Sci. Nutr.* **2021**, *9*, 728–735. [[CrossRef](#)] [[PubMed](#)]
46. Yao, J.; Liu, J.; He, Y.; Liu, L.; Xu, Z.; Lin, X.; Liu, N.; Kai, G. Systems pharmacology reveals the mechanism of Astragaloside IV in improving immune activity on cyclophosphamide-induced immunosuppressed mice. *J. Ethnopharmacol.* **2023**, *313*, 116533. [[CrossRef](#)]
47. Su, L.; Li, X.; Guo, Z.; Xiao, X.; Chen, P.; Zhang, J.; Mao, C.; Ji, D.; Mao, J.; Gao, B.; et al. Effects of different steaming times on the composition, structure and immune activity of Polygonatum Polysaccharide. *J. Ethnopharmacol.* **2023**, *310*, 116351. [[CrossRef](#)]
48. Wang, Z.; Cai, T.; He, X. Characterization, sulfated modification and bioactivity of a novel polysaccharide from *Millettiadielsiana*. *Int. J. Biol. Macromol.* **2018**, *117*, 108–115. [[CrossRef](#)]
49. Shakhmatov, E.G.; Makarova, E.N.; Belyy, V.A. Structural studies of biologically active pectin-containing polysaccharides of pomegranate *Punica granatum*. *Int. J. Biol. Macromol.* **2019**, *122*, 29–36. [[CrossRef](#)]
50. Yao, H.-Y.-Y.; Wang, J.-Q.; Yin, J.-Y.; Nie, S.-P.; Xie, M.-Y. A review of NMR analysis in polysaccharide structure and conformation: Progress, challenge and perspective. *Food Res. Int.* **2021**, *143*, 110290. [[CrossRef](#)]
51. Ren, T.; Xu, M.; Zhou, S.; Ren, J.; Li, B.; Jiang, P.; Li, H.; Wu, W.; Chen, C.; Fan, M.; et al. Structural characteristics of mixed pectin from ginseng berry and its anti-obesity effects by regulating the intestinal flora. *Int. J. Biol. Macromol.* **2023**, *242*, 124687. [[CrossRef](#)] [[PubMed](#)]
52. Chen, Y.; Jiang, X.; Xie, H.; Li, X.; Shi, L. Structural characterization and antitumor activity of a polysaccharide from ramulus mori. *Carbohydr. Polym.* **2018**, *190*, 232–239. [[CrossRef](#)] [[PubMed](#)]
53. Zhao, P.; Li, X.; Wang, Y.; Yan, L.; Guo, L.; Huang, L.; Gao, W. Characterisation and saccharide mapping of polysaccharides from four common *Polygonatum* spp. *Carbohydr. Polym.* **2020**, *233*, 115836. [[CrossRef](#)] [[PubMed](#)]
54. Ding, J.; Du, H.; Tan, H.; Li, J.; Wang, L.; Li, L.; Zhang, Y.; Liu, Y. Optimization of protein removal process of *Lonicera japonica* polysaccharide and its immunomodulatory mechanism in cyclophosphamide-induced mice by metabolomics and network pharmacology. *Food Sci. Nutr.* **2023**, *11*, 364–378. [[CrossRef](#)] [[PubMed](#)]
55. Kay, M.M.; Mendoza, J.; Diven, J.; Denton, T.; Union, N.; Lajiness, M. Age-related changes in the immune system of mice of eight medium and long-lived strains and hybrids. I. Organ, cellular, and activity changes. *Mech. Ageing Dev.* **1979**, *11*, 295–346. [[CrossRef](#)] [[PubMed](#)]
56. Lin, C.; Zhang, H.; Chen, L.; Fang, Y.; Chen, J. Immunoregulatory function of Dictyophoraechinovolvata spore polysaccharides in immunocompromised mice induced by cyclophosphamide. *Open Life Sci.* **2021**, *16*, 620–629. [[CrossRef](#)] [[PubMed](#)]

57. Huang, R.; Shen, M.; Yu, Y.; Liu, X.; Xie, J. Physicochemical characterization and immunomodulatory activity of sulfated Chinese yam polysaccharide. *Int. J. Biol. Macromol.* **2020**, *165*, 635–644. [[CrossRef](#)]
58. Zhou, X.-Q.; Chang, Y.-Z.; Ji, B.; Zhao, H.-Y.; Shen, C.-Y.; Chang, R. Efficacy of gecko polysaccharide on suppressed immune response induced by cyclophosphamide in mice. *J. Tradit. Chin. Med.* **2021**, *41*, 539–545.
59. Lee, J.-S.; Oka, K.; Watanabe, O.; Hara, H.; Ishizuka, S. Immunomodulatory effect of mushrooms on cytotoxic activity and cytokine production of intestinal lamina propria leukocytes does not necessarily depend on  $\beta$ -glucan contents. *Food Chem.* **2011**, *126*, 1521–1526. [[CrossRef](#)]
60. Zhang, N.; Liu, J.; Guo, X.; Li, S.; Wang, F.; Wang, M. *Armillaria luteo-virens* Sacc Ameliorates Dextran Sulfate Sodium Induced Colitis through Modulation of Gut Microbiota and Microbiota-Related Bile Acids. *Nutrients* **2021**, *13*, 3926. [[CrossRef](#)]
61. Zhao, W.; Chen, Y.; Tian, Y.; Wang, Y.; Du, J.; Ye, X.; Lu, L.; Sun, C. Dietary supplementation with *Dendrobium officinale* leaves improves growth, antioxidant status, immune function, and gut health in broilers. *Front. Microbiol.* **2023**, *14*, 1255894. [[CrossRef](#)] [[PubMed](#)]
62. Vornewald, P.M.; Forman, R.; Yao, R.; Parmar, N.; Lindholm, H.T.; Lee, L.S.K.; Martín-Alonso, M.; Else, K.J.; Oudhoff, M.J. Mmp17-deficient mice exhibit heightened goblet cell effector expression in the colon and increased resistance to chronic *Trichuris muris* infection. *Front. Immunol.* **2023**, *14*, 1243528. [[CrossRef](#)] [[PubMed](#)]
63. Munyaka, P.M.; Echeverry, H.; Yitbarek, A.; Camelo-Jaimes, G.; Sharif, S.; Guenter, W.; House, J.D.; Rodriguez-Lecompte, J.C. Local and systemic innate immunity in broiler chickens supplemented with yeast-derived carbohydrates. *Poult. Sci.* **2012**, *91*, 2164–2172. [[CrossRef](#)] [[PubMed](#)]

**Disclaimer/Publisher’s Note:** The statements, opinions and data contained in all publications are solely those of the individual author(s) and contributor(s) and not of MDPI and/or the editor(s). MDPI and/or the editor(s) disclaim responsibility for any injury to people or property resulting from any ideas, methods, instructions or products referred to in the content.